EFFECTS OF ARCHITECTURAL VARIABILITY ON THERMO-MECHANICAL PROPERTIES OF CERAMIC MATRIX COMPOSITES

M. B. Goldsmith[1], B. V. Sankar[1*], R. T. Haftka[1]

[1]*Department of Mechanical & Aerospace Engineering, University of Florida, PO Box 116250, University of Florida, Gainesville, FL 32611, USA.*
**sankar@ufl.edu*

Keywords: ceramic matrix composites, uncertainty, voids

Abstract

The objectives of this paper are to identify important architectural parameters that describe the SiC/SiC five harness-satin weave composite and characterize the statistical distributions and correlations of parameters from photomicrographs of cross sections; generate artificial specimens of a 2D representative volume element (RVE) of the composite; and determine the effects of architectural variability on thermo-mechanical properties. Using statistical information about the composite architecture allows for the voids to be generated and explicitly modeled in a realistic manner. Finite element analysis is used to obtain insight into the variability of the thermo-mechanical properties caused by variability of the architectural parameters.

1 Introduction

Woven ceramic matrix composites (CMCs) are candidate materials for future hypersonic vehicle systems such as thermal protection and aero-propulsion systems. Preliminary evaluation of these materials indicates that there is considerable variability in their mechanical properties. A major feature contributing to this is the randomly distributed and shaped voids, which is caused by randomness in the architecture produced at various stages in manufacturing [1-3]. Some of these uncertainties include constituent volume fractions, tow size, and tow spacing.

Conventional design methodologies compensate for the aforementioned uncertainties by use of a safety factor, which may not allow a designer to take full advantage of the composite properties because the details of the microstructure are not rigorously accounted for. In order to account for the voids in the geometry, variability at the constituent level and probabilistic techniques can be used to determine the variability in mechanical properties. The advantage of probabilistic techniques is that they account for variation in a realistic manner that may lead to a thorough representation of the model's variability. Such approaches require complete characterization of uncertainties in the composite. Thus there is a need to develop methods to model realistic uncertainties from the primitive variables, e.g., fiber and matrix properties and porosity, to the response variables such as the stiffness of the composite material [4].

In this paper, a methodology is presented for modeling the variability in architectural parameters of a 5HS CVI (five harness satin weave, chemical vapor infiltrated) SiC/SiC composite, using 2D micrographs of three specimens to identify the important architectural parameters and their distributions. Artificial specimens are generated with variability similar to that found in the composite. Finite element micromechanics simulations are then utilized to predict the variability in mechanical properties.

2 Analysis Description

2.1 Geometric Parameterization and Model Assumptions

The composite system under investigation is a SiC/SiC 5HS composite. The image in Figure 1 is a 3D representation of the weave for a 5HS unit cell [10]. The microstructure of the composite has been shown to have significant randomness, resulting in large variability in the mechanical properties. A 2D image of one cross section of the composite, obtained by Bonacuse, et al. is shown in Figure 2 [5]. The black areas in the interior of the cross section represent voids, which vary in location, size, and shape. Other 2D cross sections are not identical to the one shown, but rather, exhibit different random distributions of the voids and the microstructural characteristics such as tow size, shape, and spacing. Therefore, some simplifying assumptions, explained in the following paragraphs, were made to develop an understanding of the composite at a basic level.

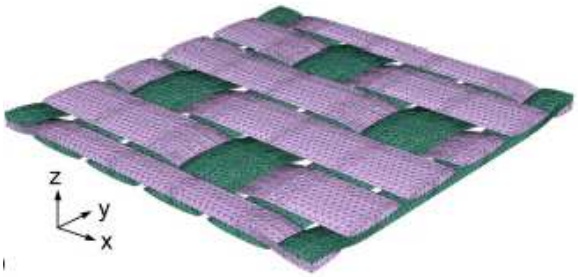

Figure 1: 3D representation of 5 HS composite [10]

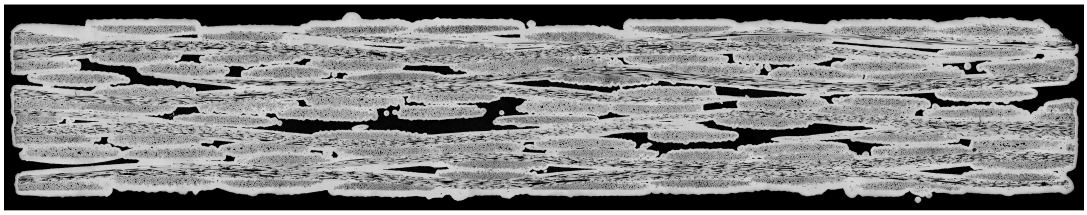

Figure 2: 2D cross section of the SiC/SiC composite microstructure

For this work, the focus was on modeling an RVE of the 8 ply 5 HS composite in order to keep the size of the problem tractable while capturing the important statistical characteristics. Preliminary work by the authors involved the use of only one unit cell, which consists of a weft tow crossing over four warp tows, as shown in Figure 3 [6]. The weave of one 2D unit cell consists of five elliptical transverse tows (shown in green in Figure 3), and one longitudinal tow that follows a sinusoidal curve (shown in blue in Figure 3). The configuration of the unit cell is based on tow spacing in the in-plane and transverse directions (Δx and Δy, respectively), transverse tow width (w), transverse tow height (h), longitudinal tow amplitude (A), longitudinal tow wavelength (λ), and crimp angle (α), as labeled in Figure 4.

After the tows are placed, the matrix is grown uniformly around the tows, until a prescribed matrix volume fraction is reached (shown in red in Figure 3). While the non-uniform matrix distribution seen in Figure 2 is not captured precisely, the method approximates the manufacturing process of matrix deposition in that the voids generated are a result of the tow placement [5]. However, the unit cell neglected the presence of any ply shifting (uneven tow alignment) that is exhibited in the actual composite, resulting in artificial specimens that did not realistically represent the void geometry. All voids were small and square-like, as opposed to a few having a large aspect ratio. The ply shifting is one cause of the voids with large aspect ratios.

In order to capture the ply shifting a larger RVE was modeled, made up of two unit cells with a uniform ply shifting for all RVEs. With more plies, the ply shifting would change within each layer. This aspect is currently being neglected since it cannot be rigorously quantified in the same manner as the other variables being investigated. The 2D representation of a 5HS RVE is shown in Figure 5. The figure is a result of using two unit cells, with one flipped upside down, and shifted by one tow length.

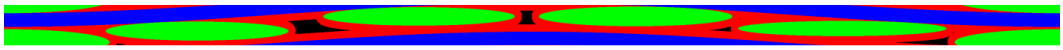

Figure 3: 2D Unit cell of 5HS composite

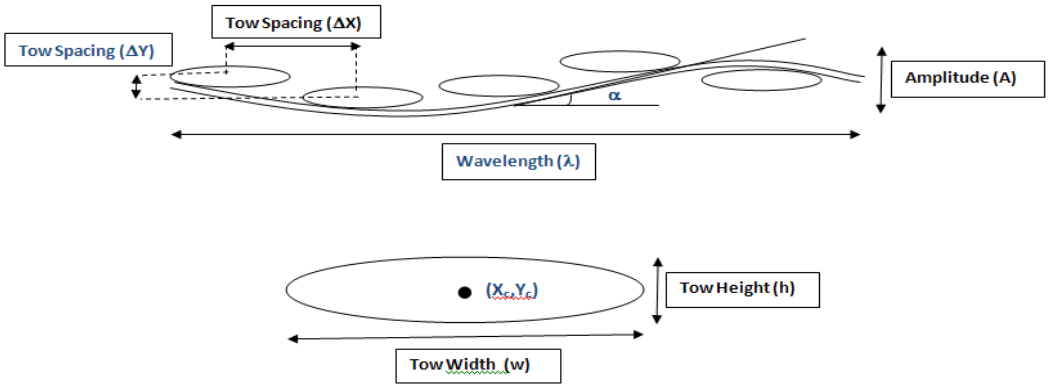

Figure 4: Geometry of unit cell

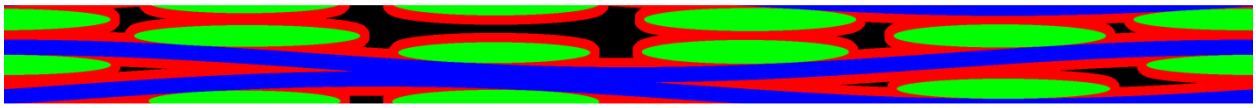

Figure 5: Example of a randomly generated RVE

2.2 Statistical Distributions and Correlations

The parameters chosen to be randomly varied were selected based on whether or not statistical data was currently available for those parameters, and whether or not there was remarkable variation. It was desired to only randomize the parameters that had quantifiable randomness, with as little guess work involved as possible. Image processing techniques were used to extract information about the tows [7]. The geometric parameters in which statistical data was available were transverse tow width (*w*), transverse tow height (*h*), and transverse tow spacing in the longitudinal direction (*s*), as labeled in Figure 6. Other architectural parameters, such as tow spacing in the through thickness ("3") direction and longitudinal tow amplitude (the difference between the maximum and minimum height of the longitudinal tow) are either dependent on the variables used, or were approximated based on visually fitting the

geometry to the specimens. The variables that do not yet have statistical data were held constant.

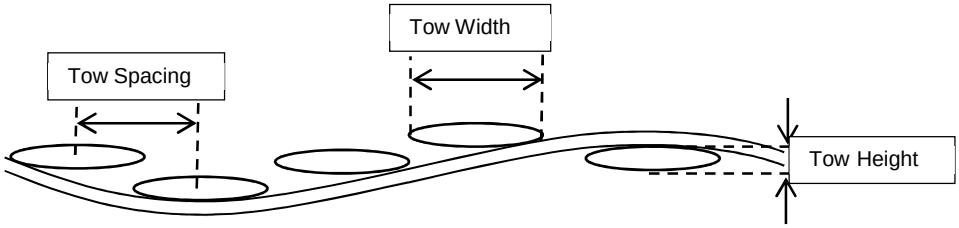

Figure 6: Definition of geometric parameters used

The random generation of the fifteen variables was based on the statistical data in three different specimens (similar to that shown in Figure 2), resulting in 240 data points. It was found that the tow spacing, tow width, and tow height fit to a normal distribution. The parameters of the distribution are given in Table 1. An issue that further complicates the problem is that the variables not only vary between the specimens, but they have a variation within each specimen as well. For this reason, correlation coefficients (a measure of the strength of the linear relationship between two variables) were accounted for during the generation of variables. Using correlation coefficients ensured that inherent architecture variation due to the manufacturing process would be accounted for and the generation of unrealistic specimens would be minimized. Therefore, each transverse tow is assigned an individual, but correlated, tow width, tow height, and tow spacing. Since there are five tows in the RVE, this results in a total of fifteen variables (five tow widths, five tow heights, and five tow spacings).

2.3 Generation of Artificial Specimens

For the finite element analysis, which is used to determine the magnitude of thermo-mechanical property variability, 38 artificial specimens were generated. The number of specimens needed is based on ongoing work involving response surfaces, not discussed here. A typical artificial specimen was shown in Figure 5.

A summary of the characteristics of the specimens generated for the three sample specimens from which the statistics were obtained is presented in Table 1. For the individual specimens, the mean and standard deviation of width, spacing and height is provided, with standard deviations in parentheses. Table 2 presents characteristics of the artificial specimens. The volume fractions and geometric parameters of tow width (w), tow spacing (s), and tow height (h) are in good agreement from the actual composite to the artificial specimens.

	% Void	**% Matrix**	**% Tow**	**w (mm)**	**s (mm)**	**h (mm)**
Specimen 1	3.2	33.8	63.0	1.14 (0.08)	1.27 (0.05)	0.12 (0.01)
Specimen 2	4.8	32.4	62.8	1.15 (0.08)	1.27 (0.06)	0.12 (0.01)
Specimen 3	3.5	32.6	63.9	1.14 (0.08)	1.27 (0.05)	0.12 (0.01)
Mean Value	3.8	32.9	63.2	1.14	1.27	0.12
St. Dev.	0.9	0.8	0.6	0.08	0.05	0.01

Table 1: Summary of volume fractions and geometric characteristics for 3 real sample specimens

	% Void	% Matrix	% Tow	w (mm)	s (mm)	h (mm)
Mean Value	4.2	32.9	62.9	1.15	1.27	0.12
St. Dev.	0.7	0.5	0.9	0.09	0.05	0.01

Table 2: Summary of volume fractions and geometric characteristics for 34 specimens

The correlation coefficients of the significantly correlated parameters (correlation parameter is greater than 0.4) are displayed in Table 3. The statistical significance is in parentheses (the likelihood of being incorrect). The correlations are determined based on 24 data points. It is likely that the spacing and width have some degree of correlation because when the composites are manufactured they are restricted to a certain width. Therefore, depending on the tow sizes, the spacing has to adjust to accommodate for all of the tows.

	Spacing 3	Spacing 4	Spacing 5	Width 3	Width 5
Spacing 1	-0.47 (0.02)				
Spacing 2	-0.42 (0.05)				0.41 (0.05)
Spacing 3		0.45 (0.05)			
Spacing 4			0.60 (0.01)		
Width 1				0.56 (0.01)	0.41 (0.05)
Width 3					0.44 (0.05)

Table 3: Comparison of correlation coefficients for real and artificial specimens

2.4 Finite Element Analysis

The RVEs were generated as red, green, and blue images with Python code (e.g. Figure 5), which were then meshed with open source software, OOF2 [8]. This mesh is then imported into commercial software, ABAQUS, for finite element analysis [9]. A combination of triangular and quadrilateral plane strain elements was used. The material properties assigned were determined by Mital, et al. [10] and are shown in Table 4. The yarn/matrix interphase is not explicitly modeled in the present study. The tows are modeled as homogenous orthotropic materials, with resultant properties based on the fiber, matrix, voids, and interphase in the tows. The matrix is an isotropic material.

	Transverse Tow	**Longitudinal Tow**	**Matrix**
E_1 **(GPa)**	106	259	420
E_2 **(GPa)**	259	106	420
E_3 **(GPa)**	106	106	420
ν_{12}	0.21	0.21	0.17
ν_{13}	0.21	0.18	0.17
ν_{23}	0.18	0.21	0.17
G_{12} *(GPa)*	41.4	41.4	179.5
G_{13} *(GPa)*	414	42.5	179.5
G_{23} *(GPa)*	42.5	41.4	179.5
α **(**10^{-6}**/°C)**	4.6	4.6	4.7

Table 4: Constituent Material Properties

In order to determine the effective elastic moduli and Poisson's ratios of the RVE based on the finite element analysis, the relationships,

$$\begin{Bmatrix}\sigma_1\\ \sigma_2\\ \sigma_3\end{Bmatrix}=\begin{bmatrix}C_{11} & C_{12} & C_{13}\\ C_{21} & C_{22} & C_{23}\\ C_{31} & C_{32} & C_{33}\end{bmatrix}\begin{Bmatrix}\varepsilon_1-\alpha_1\Delta T\\ \varepsilon_2-\alpha_2\Delta T\\ \varepsilon_3-\alpha_3\Delta T\end{Bmatrix} \quad (1)$$

$$[C]^{-1}=\begin{bmatrix}S_{11} & S_{12} & S_{13}\\ S_{21} & S_{22} & S_{23}\\ S_{31} & S_{32} & S_{33}\end{bmatrix}=\begin{bmatrix}\frac{1}{E_1} & \frac{\nu_{21}}{E_2} & \frac{\nu_{31}}{E_3}\\ \frac{\nu_{12}}{E_1} & \frac{1}{E_2} & \frac{\nu_{32}}{E_3}\\ \frac{\nu_{13}}{E_1} & \frac{\nu_{23}}{E_2} & \frac{1}{E_3}\end{bmatrix} \quad (2)$$

were used, requiring seven analyses for each specimen (three for normal moduli, three for shear moduli, and one for CTE). Periodic boundary conditions were implemented for all analyses to simulate the repetition of the RVE [11]. The stiffness matrix [*C*] is found by first applying a non-zero strain, $\varepsilon_{1,}$ keeping all other strains equal to zero. In addition, there is no thermal gradient. By volume averaging each of the three stress (σ_1, $\sigma_{2,}$ σ_3), the first column of the stiffness matrix is found. This is repeated in a similar manner for the second, third, and sixth column (a special method described below was used for determining C44 and C55). To obtain the third column, generalized plane strain (rather than plane strain) elements were used so that a non-zero strain could be applied.

Shear strain cannot be directly applied in the plane strain direction as can be done with normal strain using generalized plane strain elements. Instead, a method is used in which shell elements are implemented, providing degrees of freedom in the in-plane direction. Then, all nodes are restricted from displacement in the 1 and 3 directions, while shear strain is applied in the 12 and 23 directions. Since ABAQUS does not provide shear stress for the 12 and 23 directions with shell elements, the displacement at each node combined with shape functions can be used to extract the stress in each element manually. The method was implemented for a sample problem with a bi-material plate consisting of two isotropic materials and was shown to agree exactly.

In order to determine the coefficient of thermal expansion (CTE), total strain was not allowed, while a ΔT of 100 K was applied. The stresses were then volume averaged and the relationship in Equation 1 was used to determine the thermal expansion in the 1, 2, and 3 directions.

4 Results

The thermo-mechanical properties of 38 artificial specimens were determined with finite element analysis as described in the previous section. The mean and standard deviation of the thermal-mechanical properties are shown in Table 5. It is known that voids have a significantly more detrimental effect on the out of plane moduli than the in-plane moduli for varying void content as well as for flat shapes [12]. Therefore it is not surprising that with varying geometry, which inherently alters the void volume fraction, the coefficient of variation in the through thickness modulus is almost three times that of the coefficient of

variation in in-plane modulus. Huang and Talreja also observed that the voids would have the most significant impact in the out-of-plane shear modulus (G_{13}), which is also observed here. While the out-of-plane CTE is smaller than that of the in-plane CTE, the coefficients of thermal expansion were shown to be insensitive to the variations in architectural parameters. This is due to the fact that the coefficients of thermal expansion of the constituents are approximately the same. If the coefficients of thermal expansion were drastically different between the constituents, there would be more variability due to architectural variation.

	E_1 (GPa)	E_3 (GPa)	ν_{12}	ν_{13}	ν_{23}	G_{12} (GPa)	G_{13} (GPa)	G_{23} (GPa)	α_1 (10^{-6}/°C)	α_3 (10^{-6}/°C)
Mean	231	105.8	0.174	0.202	0.123	74.5	20.6	44.8	4.65	4.62
Std. Dev.	5	6.2	0.005	0.004	0.006	5.2	3.6	1.7	0.001	0.001

Table 5: Summary of FEA results

While the variability captured by the analysis of the RVE is large for a few material properties, the RVE is not capturing all of the variability that is thought to be present. For example, earlier work by Bonacuse, Goldberg, and Mital showed a variation in through thickness modulus from 39-103 GPa [5]. The variability of that magnitude is thought to be due to effects of variation in ply shifting, which has been neglected for the presented work.

5 Conclusions

The goal of this work was to select an RVE with architectural parameters that could be varied to effectively represent the variation in the properties of SiC/SiC composite, while also gaining an understanding of what geometric parameters were influential in determining the mechanical properties. The method of artificially generating specimens by using statistical information from the micrographs of actual composite specimens works well. The statistics of the real and artificially generated specimens are in agreement.

The RVE was characterized by varying tow widths, heights, and spacing, resulting in variability of 2-6% of the mean for normal moduli and 4-17% of the mean for shear moduli. A negligible amount of variability was found for the CTE, due to a lack of CTE mismatch in the constituents. The variability was highest for the out-of-plane tensile modulus (E_3), out-of-plane shear modulus (G_{13}), and in-plane shear modulus (G_{12}).

FEA analysis of real composite specimens revealed that there is more variability present than the variability predicted by the RVE with uniform ply shifting chosen. It is hypothesized that the variability in ply shifting should not be neglected since it may contribute to a significant portion of the variability. Future work will include a study of the effects of ply shifting on the voids shape and size, with an attempt to predict the moduli based on the voids' characteristics.

Acknowledgements

The funding for this work was provided by the NASA Graduate Student Research Program, grant number NNX10AM49H. The authors are thankful to Kim Bey of NASA LaRC and Robert Goldberg of NASA GRC for many helpful discussions. Also, thanks to Peter Bonacuse of NASA GRC for the code for model generation as well as the parameter sample

distributions, and to Subodh Mital of The University of Toledo and NASA GRC for helpful discussions regarding finite element modeling and OOF2.

References

[1] Shah, A.R., Murthy, P.L., Mital, S.K.& Bhatt, R.T. "Probabilisitc Modeling of Ceramic Matrix Composite Strength." Journal of Composite Materials. 34. 670-688. (2000).

[2] Murthy, P.L., Mital, S.K., Shah, A.R. "Probabilistic Micromechanics and Macromechanics for Ceramic Matrix Composites." NASA/TM 1997-4766. (1997).

[3] DiCarlo, J.A., Yun, H.M., Morscher, G.N., Bhatt, R.T. "SiC/Sic Composites for 1200 Degrees Farenheit and Above." NASA/TM 2004-213048. (2004).

[4] Smarslok, B., Haftka, R. & Ifju, P. "A Correlation Model for Graphite/Epoxy Properties for Propagating Uncertainty in Strain Response" in Proceedings of *23rd Technical Conference of the American Society for Composites*. Memphis, TN, USA, (2008).

[5] Bonacuse, P.J., Goldberg, R.K., Mital, S.K. "Characterization of the As-Manufactured Variability in a CVI SiC/SiC Woven Composite" in Proceedings of *ASME Turnbo Expo*, Vancouver, BC, Canada, (2011).

[6] Goldsmith, M.B., Sankar, B.V., Haftka, R.T., Goldberg R.K. "Effects of Microstructural Variability on the Mechanical Properties of Ceramic Matrix Composites" in Proceeding of *American Society for Composites 26th Technical Conference*, Montreal, QC, Canada, (2011).

[7] Goldberg, Robert K.; Bonacuse, Peter J.; Mital, Subodh K. "Investigation of Effects of Material Architecture on the Elastic Response of a Woven Ceramic Matrix Composite." NASA/TM 2012-217269. (2012).

[8] Reid, A. et.al. "Modeling Microstructures with OOF2." Int. J. Materials and Product Technology 35. 361-373. (2009).

[9] "ABAQUS version 6.9." http://www.simulia.com/products/abaqus_fea.html.

[10] Mital, S.K., Goldberg, R.K., & Bonacuse, P.J. "Two-Dimensional Nonlinear Finite Element Analysis of CMC Microstructures" in Proceedings of *ASME Turnbo Expo*, Vancouver, BC, Canada, (2011).

[11] R.V. Marrey and B.V. Sankar. "Micromechanical Models for Textile Structural Composites", NASA Contractor Report 198229. (1995)

[12] Huang, H. & Talreja, R. "Effects of void geometry on elastic properties of unidirectional fiber reinforced composites." Composites Science and Technology. 65. 1964-1981. (2005).